A R C H I V E S O F M E T A L L U R G Y A N D M A T E R I A L S
Volume 60 2015 Issue 3
DOI: 10.1515/amm-2015-0321

J. ADAMUS*,#, K. DYJA*, M. MOTYKA**

EXPERIMENTAL AND THEORETICAL DETERMINATION OF FORMING LIMIT CURVE

DOŚWIADCZALNO-TEORETYCZNE WYZNACZANIE KRZYWEJ ODKSZTAŁCEŃ GRANICZNYCH

The paper presents a method for determining forming limit curves based on a combination of experiments with finite element analysis. In the experiment a set of 6 samples with different geometries underwent plastic deformation in stretch forming till the appearance of fracture. The heights of the stamped parts at fracture moment were measured. The sheet - metal forming process for each sample was numerically simulated using Finite Element Analysis (FEA). The values of the calculated plastic strains at the moment when the simulated cup reaches the height of the real cup at fracture initiation were marked on the FLC. FLCs for stainless steel sheets: ASM 5504, 5596 and 5599 have been determined. The resultant FLCs are then used in the numerical simulations of sheet - metal forming. A comparison between the strains in the numerically simulated drawn - parts and limit strains gives the information if the sheet - metal forming process was designed properly.

Keywords: formability, forming limit curve, sheet, stainless steel

Duże znaczenie procesów tłoczenia blach w przemyśle wynika z faktu, że umożliwiają one produkcję różnych elementów od drobnej galanterii metalowej po duże elementy karoserii samochodowych i poszyciowe elementy samolotów. Ze wzrostem zapotrzebowania na wyroby tłoczone rośnie znaczenie umiejętności przewidywania zachowania się blachy podczas procesu kształtowania. W tym celu wykorzystuje się krzywe odkształceń granicznych, które stanowią granicę, powyżej której następuje pękanie wytłoczek. Najczęściej, mimo wielu trudności, krzywe odkształceń granicznych wyznacza się doświadczalnie poprzez pomiar odkształcenia materiału blachy. Chociaż dzisiaj są dostępne nowoczesne, optyczne systemy pomiarowe, to wyznaczanie krzywych odkształceń granicznych dla niektórych materiałów, takich jak: wysokowytrzymałe stopy tytanu czy analizowane w pracy wysokowytrzymałe i odporne na korozję stale stosowane w przemyśle lotniczym, nadal stanowi problem. Dlatego autorzy pracy w celu wyznaczenia KOG dla blach stalowych ASM 5504, 5596 i 5599 zdecydowali się na połączenie badań eksperymentalnych z analizą elementów skończonych.

W tym celu zestaw 6 wykrojek o zróżnicowanej geometrii poddano tłoczeniu za pomocą sztywnego, półkulistego stempla aż do pojawienia się pęknięcia wytłoczek. W momencie pękania rejestrowano głębokość wytłoczenia. Następnie modelowano proces kształtowania tych wytłoczek przy użyciu metody elementów skończonych. Obliczone wartości odkształceń w momencie, gdy symulowane wytłoczki osiągały głębokość wytłoczek rzeczywistych w momencie ich pękania naniesiono na wykres odkształceń granicznych w układzie maksymalnych (oś Y) i minimalnych (oś X) odkształceń głównych. Tak wyznaczone krzywe odkształceń granicznych służą ocenie przydatności blachy do procesów tłoczenia.

1. Introduction

Sheet - metal forming processes are of vital importance to a wide range of industries because drawn - components are both light and strong, and therefore enable a significant reduction in construction weight. It is especially important for automotive [1] and aerospace [2-4] industries where lighter vehicles mean lower fuel consumption, costs and emissions. Therefore, the demand for drawn - parts grows year by year. Large monolithic units (casts) are replaced by light sheet - metal assemblies increasingly more often. Therefore, the assessment of sheet usefulness for sheet - metal forming and determining the safe limit strains is very important. Strain - hardening exponent *n*, normal anisotropy ratio *r* and the ratio of yield strength to tensile strength R_e/R_m are the most essential parameters describing sheet formability [5-11]. Formability is defined as the sheet - metal ability to be formed into a specific shape without failure. To design cylindrical drawn - parts it is enough to know limit drawing ratio (*LDR*), which is defined as the ratio of the maximum blank diameter to the punch diameter without fracture. While forming non-symmetrical drawn -

* CZESTOCHOWA UNIVERSITY OF TECHNOLOGY, 69. DABROWSKIEGO STR., 42-201 CZESTOCHOWA, POLAND
** RZESZOW UNIVERSITY OF TECHNOLOGY, 12 POWSTAŃCÓW WARSZAWY AV., 35-959 RZESZOW, POLAND
# Corresponding author: janina.adamus@gmail.com

parts such automobile body parts, which are formed in one operation, there is no single indicator of formability because process parameters such as strain state, flow velocity and frictional conditions vary depending on the area of the drawn - part.

There are many criteria for determining fracture moment. According to them, fracture appears when a function depending on stress and strain has a certain critical value. Most of the criteria are based on the concentration of plastic strains [12-14]. From a variety of methods of formability investigation, especially in relation to complex drawn - parts, the concept of a forming limit diagram – FLD (also known as a forming limit curve - FLC) seems to be very valuable [15-18]. FLC was developed by Keeler and Backofen [19] and Goodwin [20] and presently it has become a standard characteristic in the optimisation of sheet-metal forming processes [21]. According to [22] FLC describes local necking and tearing that is a material property curve dependent on the strain state, but not on the boundary conditions. Thus the aim of sheet-metal forming design is to guarantee that strains in the sheet do not approach this limit curve. [23-27], underline that a safe forming zone with an appropriate margin between it and the limit curve must be identified just in case there are some slight changes in the material properties or process conditions. Most works discuss empirical methods to determine FLC, but with the advent of computational techniques, numerical models based on ductile fracture criteria to predict FLCs [12,28,29] appear increasingly more often. Other models, such as: diffuse necking by Swift [28], localized necking introduced by Hill [31], the thickness imperfection model developed by Marciniak and Kuczynski [32] are also used. Nevertheless, predicting FLCs involves complex calculations so that their use in practice is limited. What is more, a universal model possible to apply to various sheet metals has not been elaborated yet.

2. Forming limit curve and its role in assessment of sheet formability

A forming limit curve is a graphical representation of limit strains which cannot be exceeded during sheet - metal forming. It is presented in the system of the in - plane principal strains: major strain $\varphi 1$ and minor strain $\varphi 2$. A forming limit curve minimum occurs at or near the major strain axis. Marciniak et al [22] notices that the curve intercepts the major strain axis at approximately the value of strain - hardening exponent n. As n decreases, the height of the curve also decreases. A sheet metal exposed to strains that lie above the curve will fracture, while strains underneath the curve are safe to apply to the metal. Usually, two curves are plotted on the diagram. One of them is the Forming Limit Curve at Fracture (FLCF) and the second one, which lies slightly below FLCF, is Forming Limit Curve at Neck (FLCN). Figure 1 presents their location in FLD. The space between them is the zone where the metal can be safe or may crack, so in practice it is worth avoiding this zone. When the strains from this zone are applied to the metal, necking is likely to occur.

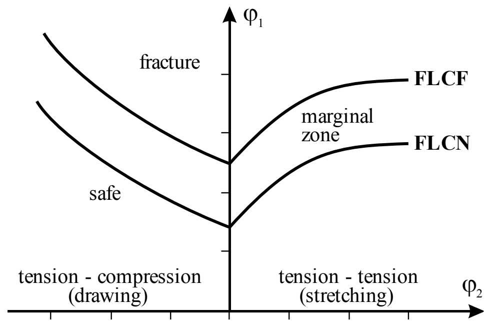

Fig. 1 Forming Limit Diagram

FLD is used in sheet - metal forming for predicting the forming behaviour of sheet metal and making a decision if any improvements in the forming process are needed. To do this the strains in the drawn - part (φ_{d-p}) are compared with the limit strains (φ_l). If the strains in the drawn - part are much smaller than the limit strains ($\varphi_{d-p} << \varphi_l$) it means that it is possible to use the sheet with lower formability. If the strains in the drawn - part are only slightly smaller than the limit strains ($\varphi_{d-p} < \varphi_l$) it means that no changes are needed. And if the strains in the drawn - part significantly exceed the limit strains ($\varphi_{d-p} \geq \varphi_l$) it is necessary to change forming conditions (e.g. improve lubrication) or choose the sheet with higher formability or introduce changes in design (e.g. increase fillet radius).

3. Determination of FLC

Generally, forming limit curves are done theoretically [2,33,34] or empirically using a series of tests. In order to simulate different strain conditions, strains are applied to metal samples of different shape in tests. The samples are usually stretched using a hemispherical punch until crack appears. Before the forming process, each sample is covered with a grid pattern, commonly a circular grid printed on the sheet metal by the electro-chemical grid marking technique. Due to plastic deformation the circles transform into ellipses. Strain values are calculated on the basis of the measurement of the circle diameter before deformation d_0, and the major d_1 and minor d_2 axes of the ellipse in the area of localised necking or fracture, as shown in Figure 2. Calculations of the major and minor strains for different strain states allow for the generation of FLD as a line at which cracking commences.

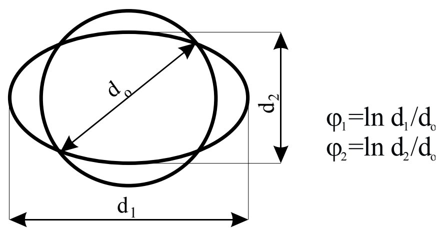

Fig. 2. Scheme of deformation measurement

FLDs are a diagnostic tool for sheet - metal strain analysis and are used for evaluating sheet - metal forming operations and material selection. Although there are some special measuring systems for strain measurements which use images taken by the system during the deformation process, comparing to a reference grid comparable to the circular grid on the metal, there are some difficulties with computing the strains for titanium alloy or nickel superalloy sheets. Firstly, this is due to the fact that it is hard to put any well-visible grid pattern on these sheet - metals, and secondly, it is difficult to measure the grid deformation because of high spring - back, which causes immediate distortion of the grid after sample unloading. Therefore, the authors decided to combine experimental tests with numerical simulations. In order to do this, a set of 6 samples, which are shown in Figure 3, were stretched over a spherical punch to crack initiation.

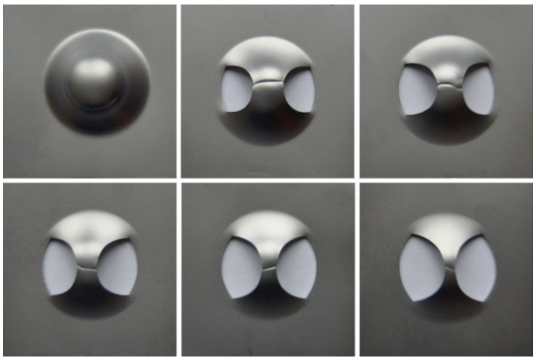

Fig. 3. Sample view after stretching over hemispherical punch

The height of the drawn - parts at crack moment was measured. Then the same forming process was simulated using Finite Element Analysis, and the major and minor strains were taken from the calculations when the drawn - part reaches the same height as the real drawn - part at crack. These strain values were used for assessing the FLDs, which had been determined using Keeler formula. Such a formula is used in a commercial PamStamp 2G code [35]. An example of a numerical calculation for the sample with lateral cut r=10 mm is shown in Figure 4.

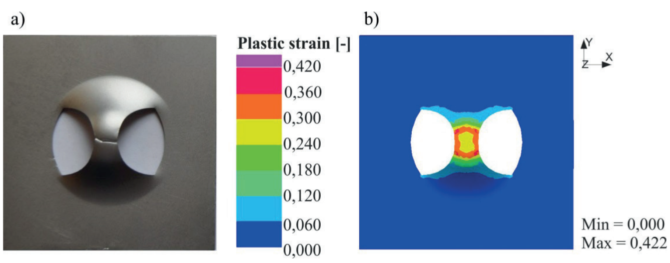

Fig. 4. Simulation results for sample with cutout r=10 mm

A numerical model, which is shown in Figure 5, reproduces the real tool.

The tool geometry was prepared using Catia v.5, and then imported to PAMStamp 2G. Both the tool and the blanks were meshed with 4-node shell elements. The boundary conditions were assigned to each part of the tool. All degrees of freedom have been taken off the die. The punch and the blank-holder can move in the Z axis. A velocity vector was applied to the punch while a force was applied to the blank-holder. The blank had all degrees of freedom.

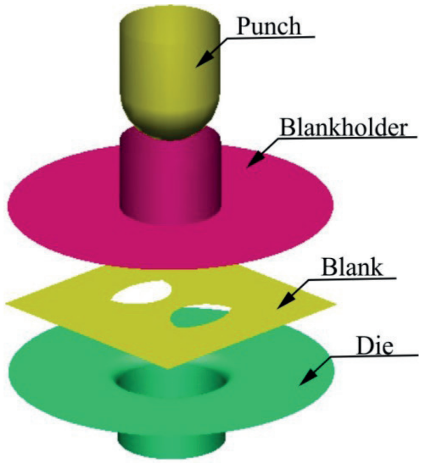

Fig. 5. Tool geometry

The following material sheets were analysed: ASM 5504 (stainless steel AISI 410) with a thickness of 0.75 mm, 5596 (Inconel 718) with a thickness of 1.27 mm and 5599 (Inconel 625) with a thickness of 0.6 mm. The chemical composition of these materials is given in Table 1. In the numerical calculations of the forming process the material data presented in Table 2 were assumed. The mechanical properties have been determined experimentally in the tensile test.

TABLE 1

Chemical composition

Element	ASM 5504	ASM 5596	ASM 5599
	weight [%]		
Al	-	0.2-0.8	0.3
B	-	0.006 max	-
C	0.15 max	0.08 max	0.05
Cu	-	0.3 max	-
Co	-	1.0 max	-
Cr	12.5	17-21	21.5
Fe	balance	17.0	2.5 max
Mn	1.0 max	0.35 max	-
Mo	-	2.8-3.3	9.0
Nb	-	4.75-5.5	3.7
Ni	-	balance 50-55	balance
P	0.04 max	0.015 max	-
S	0.03 max	0.015 max	-
Si	-	0.35 max	-
Ti	-	0.65-1.15	0.3

TABLE 2

Material data assumed in numerical calculations

Property / Material	Yield strength R_e [MPa]	Tensile strength R_m [MPa]	Elongation A [%]	Strength coefficient K [MPa]	Strain - hardening exponent n [-]
5504	287.80	517.40	43.00	918.44	0.25
5596	342.41	756.01	50.40	1358.50	0.32
5599	467.51	939.40	33.00	1582.00	0.25

The FLDs for the analysed sheet metals are presented in Figure 6.

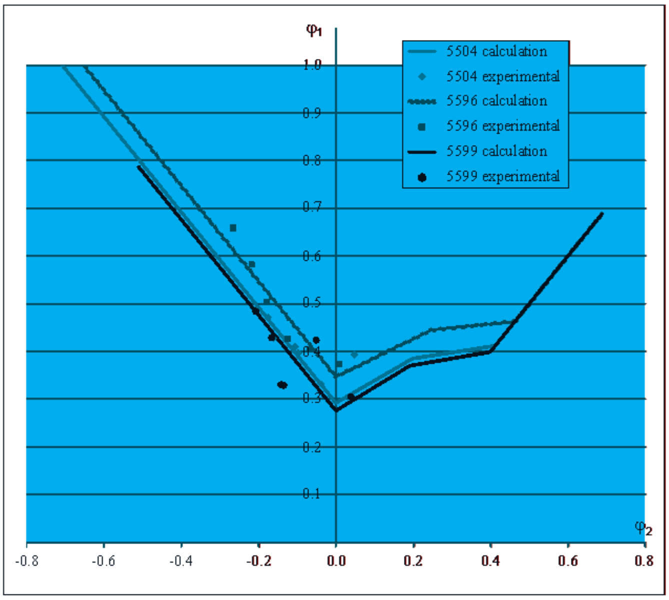

Fig. 6. Forming limit diagram for analysed sheets

Quite good convergence between the experimental and calculation results is observed. The 5596 sheet metal has the highest level of limit strains. The other curves are a little bit lower; their formability is very close. The formability of the analysed sheets is lower than typical deep drawing quality (DDQ) steels, moreover they have especially high spring - back, therefore forming these sheets at ambient temperature is difficult.

4. Summary

- Searching for the proper method of assessing sheet formability is very important due to the fact that drawn - parts production is mostly mass and each shortcoming created during fabrication causes high costs.
- The proposed method allows for determining Forming Limit Curves for sheets which are characterised by poor formability, and due to high corrosion resistance it is nearly impossible to cover them with a visible grid pattern. The method joins testing with the numerical simulation of the forming process.
- The formability of the analysed sheets is lower than typical deep drawing quality steels. The 5596 sheet has the highest level of limit strains. The other curves are a little bit lower; their formability is very close.

Acknowledgement

Financial support of Structural Funds in the Operational Programme - Innovative Economy (IE OP) financed from the European Regional Development Fund - Project “Modern material technologies in aerospace industry”, Nr POIG.01.01.02-00-015/08-00 is gratefully acknowledged.

REFERENCES

[1] H. Hayashi, T. Nakagawa, J. Mater. Process. Technol. **464**, 55-487 (1994).
[2] F. Djavanroodi, A. Derogar, Mater. Design **31,** 4866–4875 (2010).
[3] J. Adamus, P. Lacki, Comp. Mater. Sci. **94,** 66-72 (2014).
[4] P. Lacki, in: E. Onate, D.R.J. Owen, D. Peric, B.Suarez (Eds.), Computational Plasticity XII: Fundamentals and Applications **101674**, 854-861, Barcelona, Spain (2013).
[5] J. Adamus, P. Lacki, Key Eng. Mat. **549**, 31-38 (2013).
[6] J. Adamus, P. Lacki, M. Motyka, K. Kubiak, in: L. Zhou, H. Chang, Y. Lu, D. Xu (Eds.), Ti-2011 - 12th World Conference on Titanium, **1**, 337-341, Science Press Beijing, CNCC, Beijing, China (2011).
[7] A. K. Gupta, D. R. Kumar, J. Mater. Process. Technol. **172**, 225–237(2006).
[8] S. Holmberg, B. Enquist, P. Thilderkvist, J. Mater. Process. Technol. **145**,72–83 (2004).
[9] P. Lacki, J. Adamus, T. Sadowski, K. Wojsyk, M. Kneć, in: J. Eberhardsteiner, H. J. Böhm, F. G. Rammerstorfer (Eds.) ECCOMAS 2012 Congress, 4969-4979, Vienna, Austria, (2012).
[10] P. Lacki, J. Adamus, W. Wieckowski, J. Winowiecka, Arch. Metall. Mater. **58,** (1), 139-143 (2013)
[11] W. Fracz, F. Stachowicz, T. Trzepieciński, T. Pieja, Arch. Metall. Mater. **58**, (4), 1213-1217 (2013).
[12] L. Wang, T.C. Lee, Int. Mach. Tools Manuf. **46**, 988–995 (2006).
[13] M. Kuroda, V. Tvergaard, Int. J. Solids Struct. **37**, 5037–5059 (2000).
[14] S. Storen, J.R. Rice, J. Mech. Phys. Solids **23**, 421-441 (1975).
[15] S.S. Hecker, Sheet Metal. Ind. **52**, 671–676 (1975).
[16] J. Gronostajski, A. Dolny, Determination of forming limit curves by means of Marciniak punch. Memor. Sci. Rev. Metal. **4**, 570–578 (1980).
[17] R. Narayanasamy, C. S. Narayanan, Mater. Des. **29**, 1467–1475 (2008).
[18] K. S. Raghavan, Metall. Trans. A **26**, 2075–2084 (1995).
[19] S.P. Keeler, W. A. Backofen, Trans. ASM **56**, 25–48 (1963).
[20] G.M. Goodwin, SAE, no **680093**, 380-387 (1968).
[21] ASTM E2218 - 02(2008) Standard Test Method for Determining Forming Limit Curves
[22] Z. Marciniak, J.L. Duncan, S.J. Hu, Butterworth-Heinemann, London 2002.
[23] D. Banabic, H. Aretz, L. Paraianu, P. Jurco, Model. Simul. Mater. Sci. Eng. **13,** 759-769 (2005).
[24] D. Banabic, H. J. Bunge, K. Pöhland, A.E. Tekkaya, Formability of Metallic Materials. Springer, Berlin 2000.
[25] J. Slota, E. Spisak, Metalurgia **4**, 249–253 (2005).
[26] Y. M. Huang, Y. W. Tsai, C. L. Li, J. Mater. Process Technol. **201**, 385–389 (2008).
[27] J. Winowiecka, W. Wieckowski, M. Zawadzki, Comp. Mater. Sci. **77**, 108-113 (2013).
[28] H. Takuda, K. Mori, N. Hatta, J. Mater. Process. Technol. **95**, 116–121 (1999).
[29] [29] T. Pepelnjak, K. Kuzman, J. Achiev. Mater. Manuf. Eng. **20**, 375-378 (2007).
[30] H.W. Swift, J. Mech. Phys. Solids **1**, 1–18 (1952).
[31] R. Hill, Proc. Roy. Soc. London **193A,** 197–281 (1948).

[32] Z. Marciniak, K. Kuczynski, Int. J. Mech. Sci. **9**, 609–620(1967).
[33] S. Ahmadi, A. R. Eivani, A. Akbarzadeh, Comput. Mater. Sci. **44**, 1252–1257 (2009).
[34] T. B. Stoughton, X. Zhu, Int. J. Plast. **20**, 1463–86 (2004).
[35] PamStamp 2G v 2011, User's Guide.

Received: 20 December 2014.